encyclopedia

MDPI

Entry

Fundamentals of Water Radiolysis

Jean-Paul Jay-Gerin

Department of Medical Imaging and Radiation Sciences, Faculty of Medicine and Health Sciences, Université de Sherbrooke, 3001, 12th Avenue Nord, Sherbrooke, QC J1H 5N4, Canada; jean-paul.jay-gerin@usherbrooke.ca

Definition: Radiolysis of water and aqueous solutions refers to the decomposition of water and its solutions under exposure to ionizing radiation, such as γ-rays, X-rays, accelerated particles, or fast neutrons. This exposure leads to the formation of highly reactive species, including free radicals like hydroxyl radicals ($^{\bullet}OH$), hydrated electrons (e^{-}_{aq}), and hydrogen atoms ($H^{\bullet}$), as well as molecular products like molecular hydrogen (H_2) and hydrogen peroxide (H_2O_2). These species may further react with each other or with solutes in the solution. The yield and behavior of these radiolytic products depend on various factors, including pH, radiation type and energy, dose rate, and the presence of dissolved solutes such as oxygen or ferrous ions, as in the case of the ferrous sulfate (Fricke) dosimeter. Aqueous radiation chemistry has been pivotal for over a century, driving advancements in diverse fields, including nuclear science and technology—particularly in water-cooled reactors—radiobiology, bioradical chemistry, radiotherapy, food preservation, wastewater treatment, and the long-term management of nuclear waste. This field is also vital for understanding radiation effects in space.

Keywords: water and aqueous solutions; radiolysis; time scale of radiolysis events; linear energy transfer (LET); radical and molecular yields; pH; dissolved oxygen; dose rate; Fricke chemical dosimeter

Academic Editor: Michael I. Ojovan

Received: 28 January 2025
Revised: 2 March 2025
Accepted: 4 March 2025
Published: 7 March 2025

Citation: Jay-Gerin, J.-P. Fundamentals of Water Radiolysis. *Encyclopedia* **2025**, *5*, 38. https://doi.org/10.3390/encyclopedia5010038

1. Introduction: Some History

Radiation chemistry research focuses heavily on water and aqueous solutions, emphasizing their critical importance in biological systems and a variety of practical applications. This research spans fundamental scientific aspects and extends into areas such as nuclear science and technology—especially in water-cooled nuclear power reactors, where controlling radiolytic processes is crucial to prevent deleterious (corrosion) effects, radiation effects in space, radiotherapy, diagnostic radiology, and the long-term environmental management of nuclear waste materials (for a selection of articles and books published since 1980, see [1–30]). Additionally, water is the standard reference material in clinical radiation therapy, chosen for its ionizing radiation absorption properties, which closely mimic those of biological tissue [31].

Water radiolysis, the decomposition of water under ionizing radiation, has been an active research area for over a century. In fact, it is known that only a few months after the discovery of X-rays by Wilhelm C. Röntgen at the University of Würzburg, Germany, natural radioactivity was, in turn, discovered in February–May 1896 by Henri Becquerel in Paris. Following this, polonium [32] and radium [33] were identified in 1898 by Pierre and Marie Sklodowska Curie, along with Gustave Bémont. The Curies and Becquerel were awarded the Nobel Prize in Physics in 1903 for these discoveries. Early observations by Curie and Debierne [34], Giesel [35,36], and Ramsay and Soddy [37] revealed that dissolved radium salts continuously decompose aqueous solutions, releasing hydrogen

and oxygen gases primarily due to the emission of α-particles from radium, a process Marie Curie [38] compared to "electrolysis without electrodes". Notably, the pivotal experiment by Rutherford and Royds [39] providing direct evidence that alpha particles are ionized helium atoms dates from 1909.

Various other studies on the gaseous emissions resulting from the action of radon on water were subsequently conducted by Ramsay and Cameron [40,41] and by Usher [42]. These authors demonstrated that α-particles are primarily responsible for the observed chemical effects. Conversely, Kernbaum [43] found that X-rays do not produce any observable gas release under similar conditions, a finding later corroborated by Risse [44] and Fricke and Brownscombe [45]. In fact, it is now well established that α-rays induce the radiolysis of water into measurable stable products, whereas X-ray-induced radiolysis in the absence of air is notably weak due to significant and rapid reverse reactions.

Most importantly, André Debierne [46], in 1914, first suggested that water radiolysis produces hydrogen atoms ($H^{\bullet}$) and hydroxyl radicals ($^{\bullet}OH$), a hypothesis that predated the general acceptance of such reactive intermediates by about 30 years. Debierne proposed, "*On peut supposer que chaque molécule d'eau est décomposée en un atome H et un radical hydroxyl OH, deux atomes d'hydrogène se soudant pour faire une molécule d'hydrogène, et deux radicaux hydroxyls donnant lieu à la production d'une molécule d'eau oxygénée*" [One can suppose that each water molecule is decomposed into one hydrogen atom and one hydroxyl radical OH, with two hydrogen atoms bonding to form a hydrogen molecule, and two hydroxyl radicals resulting in the production of a hydrogen peroxide molecule]. Such an interpretation, founded in solid principles, was overlooked for years until Risse [47], the group led by M. Burton and J. Franck (see, e.g., [48,49]), and Weiss [50] independently stated it.

With these brief reminders in mind, we direct readers to comprehensive historical accounts of aqueous radiation chemistry published in the last few decades [51–60] for further details.

This review investigates the effects of ionizing radiation on water and dilute aqueous solutions, starting with the basics of water radiolysis. Given the breadth of this topic and space limitations, a comprehensive analysis is beyond the scope of a single manuscript. Instead, we provide a concise assessment of key parameters, including pH, radiation type and energy, dissolved solutes (e.g., oxygen), and dose rate. The review concludes with an examination of the radiolysis of the ferrous sulfate (Fricke) dosimeter under various experimental conditions. Much of the content aligns with the curriculum of the author's graduate-level *Introduction to Radiation Chemistry* course at the Université de Sherbrooke.

2. Fundamentals of Water Radiolysis

2.1. Radiolysis of Pure, Deaerated Water: Time Scale of Events and Formation of Primary Radical and Molecular Products

In condensed phases like liquid water, the initial products of radiolysis—including water cations ($H_2O^{\bullet+}$), excited water molecules (H_2O^*, where the asterisk * denotes an excited state), and ejected secondary electrons—are produced during the "physical" stage of radiation action [61,62]. The uncertainty principle ($\Delta t.\Delta E \sim \hbar$) determines the minimum time required for events involving specific energy transfers. For instance, producing a 100-eV event takes about 10^{-17} s, while generating a 10-eV event takes around 10^{-16} s (1 eV $\approx 1.602 \times 10^{-19}$ J) [7]. Furthermore, ionization of the inner K-shell of an oxygen atom, which requires approximately 532 eV, can lead to the emission of Auger electrons [11,23]. This process, combined with subsequent molecular interactions, can result in the formation of doubly ionized water cations (H_2O^{++}). Due to their high energetic and chemical instability, these species undergo a rapid sequence of reactions and rearrangements during the

subsequent "physicochemical" stage, which lasts up to ~10^{-12} s (1 picosecond) after the initial energy deposition.

When ionized into $H_2O^{\bullet+}$, water molecules become highly unstable. With a very short lifetime of ~50×10^{-15} s (50 femtoseconds) [63], they can undergo random migration through a series of resonant electron transfers—about 20, on average—spanning a few molecular diameters [64,65]. These transient $H_2O^{\bullet+}$ radical cations subsequently decompose through a pseudo-first-order proton transfer reaction with a neighboring H_2O molecule, producing hydronium ions (H_3O^+ or H^+_{aq}) and hydroxyl radicals ($^{\bullet}OH$):

$$H_2O^{\bullet+} + H_2O \rightarrow H_3O^+ + {}^{\bullet}OH. \quad (1)$$

At this stage, secondary (or "dry") electrons—initially produced in large quantities (~10^4 electrons per MeV of deposited energy) with kinetic energies predominantly below ~50–100 eV [18,66–68]—gradually slow down to subexcitation levels (below ~7.3 eV, the first electronic excitation threshold of water [69]) and eventually reach thermal energies (~0.025 eV at 25 °C). As thermalization nears, the ejected electron may quickly localize and become trapped in a pre-existing potential energy well of suitable depth within the liquid, forming a "wet" or "incompletely relaxed" electron [3,16,70]. The precise physicochemical properties of this wet electron are still being investigated. This precedes its transition to a fully relaxed, hydrated state (e^-_{aq}) within about 240 fs to 1.3 ps [71–74], as nearby molecular dipoles reorient in response to the electron's negative charge [75–77]. In liquid water at 25 °C, thermalization, trapping, and hydration then proceed in quick succession [16]:

$$e^- \rightarrow e^-_{sub} \rightarrow e^-_{th} \rightarrow e^-_{tr} \rightarrow e^-_{aq}. \quad (2)$$

As the ejected electron slows down, it may be temporarily captured resonantly by a water molecule to form a transient molecular anion. This anion primarily dissociates into H^- and $^{\bullet}OH$ according to

$$e^- + H_2O \rightarrow (H_2O^{\bullet-})^* \rightarrow H^- + {}^{\bullet}OH, \quad (3)$$

followed by a rapid proton transfer reaction, where the hydride ion reacts with another water molecule:

$$H^- + H_2O \rightarrow H_2 + OH^-. \quad (4)$$

Reaction (4), referred to as the "dissociative electron attachment" (DEA) process [78], was initially observed in condensed amorphous water at ~20 K for electron energies between 5 and 12 eV, with the maximum H^- desorption yield occurring around 7.4 eV [79].

Additionally, low-energy "dry" secondary electrons can also be recaptured by their short-lived $H_2O^{\bullet+}$ parent cations through Coulomb attraction, resulting in the formation of excited water molecules:

$$e^- + H_2O^{\bullet+} \rightarrow H_2O^* \text{ (electron–cation "geminate" recombination)} \quad (5)$$

This recombination occurs only with electrons formed near the parent water cation and happens during the initial steps of their random walk [80]. Reaction (5) must occur prior to the H_2O^+ cation undergoing reaction (1), specifically within a timescale of ~50 fs [63].

Excited water molecules can be formed either directly through an initial event [23] or via the neutralization reaction (5). Currently, the decay pathways of excited water molecules in the liquid phase and their associated branching ratios remain poorly understood. Nonetheless, the influence of water's excited states on the primary radical and molecular products during water radiolysis is relatively minor compared to ionization pro-

cesses. Consequently, the limited understanding of these states has only a minimal impact. As a result, the deexcitation mechanisms of H_2O^* are generally assumed to closely resemble those observed in isolated water molecules, as described below (see, e.g., [23,65,81]):

$$H_2O^* \rightarrow H^\bullet + {}^\bullet OH \quad (6)$$

$$H_2O^* \rightarrow H_2 + O(^1D) \quad (7)$$

$$H_2O^* \rightarrow 2H^\bullet + {}^\bullet O^\bullet(^3P) \quad (8)$$

$$H_2O^* \rightarrow H_2O + \text{release of thermal energy} \quad (9)$$

Here, $O(^1D)$ and ${}^\bullet O^\bullet(^3P)$ refer to oxygen atoms in their singlet ^1D first excited state and triplet ^3P ground state, respectively. Notably, $O(^1D)$ atoms produced in reaction (7) possess a high-energy state and react efficiently with water, forming H_2O_2 or potentially $2{}^\bullet OH$ [82,83]. In contrast, ${}^\bullet O^\bullet(^3P)$ atoms produced in reaction (8) exhibit low reactivity with water but readily react with a broad range of organic and inorganic additives in aqueous solutions [84].

An excited water molecule with energy exceeding ~6.5 eV can also undergo decomposition through a "photoionization" process [70–72,85–87], resulting in the production of a hydrated electron and a water cation, as shown in the reaction

$$H_2O^* \rightarrow e^-_{aq} + H_2O^{\bullet+} \text{ (threshold at ~6.5 eV)} \quad (10)$$

The produced $H_2O^{\bullet+}$ cation may then participate in further reactions, such as reaction (1).

It is worth noting that DEA [reactions (3) and (4)] and the decomposition of excited water resulting from the geminate recombination of the dry electron with $H_2O^{\bullet+}$ [reactions (5) and (7)] have been proposed as key mechanisms for molecular hydrogen production during the early stages of liquid water radiolysis [65,78,88–93]. Experimental evidence strongly supports these mechanisms, indicating that the traditionally accepted "nonscavengeable" H_2 yield [94]—which cannot be removed by scavenger experiments—originates from precursors of e^-_{aq} and can be significantly reduced by high concentrations of appropriate dry-electron scavengers [15]. However, the exact source of H_2 from water radiolysis at early times continues to be a subject of ongoing debate [95,96].

Another interesting aspect is that a thermalized electron, once trapped in the liquid, can engage in chemical reactions due to its localized nature before fully relaxing into the e^-_{aq} state (see, e.g., [97–101]). One such reaction is [102]

$$e^-_{tr} + H_2O \rightarrow H^\bullet + OH^-. \quad (11)$$

This reaction would occur on a timescale comparable to electron hydration, competing with it and providing a novel pathway for generating an "initial" yield of $H^\bullet$ atoms in water. At these early times, the primary source of atomic hydrogen in water radiolysis is typically the dissociation of excited water molecules, as indicated by reactions (6) and (8).

Finally, regarding the doubly charged cation H_2O^{++} left after Auger emission, it is generally believed to dissociate in solution through a two-step process involving sequential deprotonation reactions (see, e.g., [23,68,103] and cited references), namely,

$$H_2O^{++} + H_2O \rightarrow H_3O^+ + OH^+, \quad (12)$$

quickly followed by

$$OH^+ + H_2O \rightarrow H_3O^+ + O(^3P) \quad (13)$$

By ~1 ps, the various "initial" radiolysis products formed in pure, deaerated water include e^-_{aq}, H_3O^+, OH^-, $H^\bullet$, $^\bullet OH$, H_2, H_2O_2, $O(^1D)$, $^\bullet O^\bullet(^3P)$, $O^{\bullet -}$, and others, with H_3O^+, e^-_{aq}, and $^\bullet OH$ being produced in the highest concentrations. This moment marks the onset of the "chemical" stage, during which these reactive species begin diffusing away from their original formation sites. Notably, at this stage, all radiolytic species are spatially distributed within a distinct, highly nonhomogeneous "track structure" that strongly depends on the type and energy of the radiation—often referred to as "radiation quality" (see, e.g., [5,16,17,23,53,104–106]). This distribution is quantified by the "linear energy transfer" (LET), also known as "stopping power", denoted by $(-dE/dx)$. Usually, LET values are expressed in units of keV/μm [16,107].

For radiations with low LET—such as Compton electrons from ^{60}Co γ-rays, fast electrons (e.g., MeV), or a few hundred MeV protons with typical LET values around ~0.3 keV/μm—and in the absence of dose-rate effects (i.e., no track interactions), the initial track structure is composed of small, well-separated Magee-type "spurs" (clusters of radiolytic species with a nearly spherical shape) along the radiation path [16,108–110]. At this stage, radiolysis is primarily characterized by diffusion processes governed by Fick's macroscopic diffusion laws and the chemical reactions among reactive species as the tracks evolve over time. At room temperature, track expansion effectively concludes when spurs merge through diffusion, about 0.2 microseconds after the initial ionization event [111]. At this point in time, the radiation track structure has dissipated, and the species escaping spur/track reactions are homogeneously distributed throughout the solution. The main reactive species existing at homogeneity include e^-_{aq}, $H^\bullet$, and $^\bullet OH$ (the "radical" products) along with H_2 and H_2O_2 (the "molecular" products) [1,2,5,7,13,20,53]. These species are traditionally referred to as "primary" species, although this designation can be somewhat misleading, since they themselves result from a complex sequence of reactions involving species that existed prior to them [112]. Some authors [113], however, have used the term "primary" in the sense that these species are produced directly within the radiation track itself. Their yields, also known as "primary" or "escape" yields, are denoted by the lowercase symbols $g(e^-_{aq})$, $g(H^\bullet)$, $g(^\bullet OH)$, $g(H_2)$, and $g(H_2O_2)$. These yields measure the number of each species formed or consumed per 100 eV of absorbed radiation energy, remaining available after spur/track expansion to react with added solutes in dilute aqueous solutions [114]. Observed or final radiation chemical yields are always denoted by the uppercase form $G(X)$ and reported in these units. Additionally, using "molecules per 100 eV" as a unit for yields is more insightful than SI units (mol/J). In these so-called "old" units, the yield of a given species offers a good measure of the actual average number of that species present within a spur. This is particularly relevant given that the average energy deposited in a spur is about 50 to 100 eV [18,66–68]. For this reason, the author prefers these units and advocates for their continued use. However, for those who prefer SI units, the conversion relationship is given by 1 molecule/100 eV ≈ 0.10364 μmol/J [53].

Finally, beyond a few microseconds, reactions in the bulk solution can generally be described using conventional homogeneous chemistry methods (see, e.g., [115]). The time scale for various processes involved in the low-LET radiolysis of deaerated water is illustrated in Figure 1.

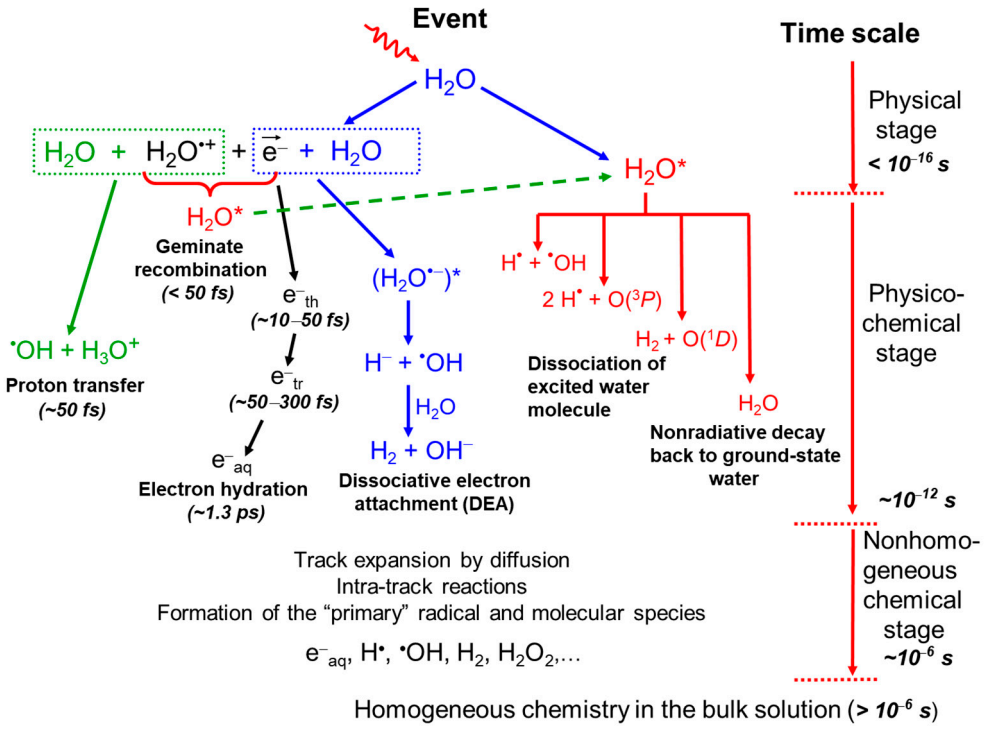

Figure 1. The time scale of events in the radiolysis of oxygen-free water at low LET. The figure is divided into three distinct consecutive stages: physical, physicochemical, and chemical, as proposed by Platzman [61] and Kuppermann [62]. Refer to the text for details. Adapted from Bepari et al. [116].

The radiolysis of pure deaerated (air-free) liquid water can be described by the following *global* equation (denoted by the symbol ~~->), written for an absorbed energy of 100 eV [23,53]:

$$g(-H_2O)\ H_2O \sim\sim> g(e^-_{aq})\ e^-_{aq} + g(H^\bullet)\ H^\bullet + g(H_2)\ H_2 + g(H_3O^+)\ H_3O^+ + g(OH^-)\ OH^- + \\ + g(^\bullet OH)\ ^\bullet OH + g(H_2O_2)\ H_2O_2 + \ldots, \quad (14)$$

where the coefficients g(X) represent the "primary" radical and molecular yields. At this stage, $g(-H_2O)$ indicates the yield associated with water decomposition. For ^{60}Co γ-rays (photons with energies of 1.17 and 1.33 MeV) or fast electrons of similar energies in neutral water at 25 °C, the reported primary yields, expressed in molecules per 100 eV, are (see, e.g., [1,5,7,17,20,117–120])

$$g(e^-_{aq}) = 2.65 \qquad g(H^\bullet) = 0.60 \qquad g(H_2) = 0.45 \\ g(^\bullet OH) = 2.80\ g(H_2O_2) = 0.68 \qquad g(-H_2O) = 4.15. \quad (15)$$

These yields, which remain pH-independent over the range of ~3–11 [2,6,11,119,121–123], are governed by the following electroneutrality and material balance relationships:

$$g(e^-_{aq}) + g(OH^-) = g(H_3O^+) \quad (16)$$

$$g(-H_2O) = g(e^-_{aq}) + g(H^\bullet) + 2g(H_2) = g(^\bullet OH) + 2g(H_2O_2). \quad (17)$$

Finally, it is important to note that molecular hydrogen, produced by radiolysis, is a gas that is largely chemically inert and tends to escape readily from the solution [124]. In this instance, oxygen can also be produced by low-LET radiation, though indirectly, as a secondary and minor radiolytic product through the following reactions [20,125]:

$$^\bullet OH + H_2O_2 \rightarrow HO_2^\bullet + H_2O \qquad k = 2.9 \times 10^7\ M^{-1}\ s^{-1} \text{ at } 25\ ^\circ C \quad (18)$$

followed by

$$^{\bullet}OH + HO_2^{\bullet} \rightarrow O_2 + H_2O \quad (19)$$

and

$$HO_2^{\bullet} + HO_2^{\bullet} \rightarrow O_2 + H_2O_2. \quad (20)$$

When H_2 is retained in the solution, as in water-cooled nuclear reactors where extra H_2 is added to the coolant to prevent corrosion of in-core components (see, e.g., [20,29,58,126] and references therein), it reacts with the oxidizing radical $^{\bullet}OH$ as follows:

$$^{\bullet}OH + H_2 \rightarrow H_2O + H^{\bullet} \quad (21)$$

with a rate constant of $k = 3.9 \times 10^7$ M^{-1} s^{-1} at 25 °C [20], 8.0×10^8 M^{-1} s^{-1} at 300 °C [127], and 1.5×10^8 M^{-1} s^{-1} at 400 °C with a pressure of 25 MPa [128].

This reaction, along with reaction (22), initiates a chain reaction—sometimes referred to as the "Allen chain reaction" [129,130]—that results in the destruction of hydrogen peroxide:

$$H^{\bullet} + H_2O_2 \rightarrow {}^{\bullet}OH + H_2O. \quad (22)$$

2.2. The Effect of Dissolved Oxygen

Oxygen is soluble in many environments, notably in water. Without taking specific precautions, the irradiated target will contain oxygen. For instance, at 1 atmosphere and 25 °C, air-saturated water contains about 2.5×10^{-4} M dissolved oxygen. This concentration increases to ~1.3×10^{-3} M in oxygen-saturated water at room temperature.

The chemistry of oxygen is fundamentally concerned with electron transfers in oxidation–reduction (redox) reactions. As a diradical, molecular oxygen possesses two unpaired electrons, enabling it to readily react with primary radicals formed during the radiolysis of aerated aqueous solutions, such as e^-_{aq} and $H^{\bullet}$ atoms. These reactions proceed as follows [5,20,53,131]:

$$O_2 + e^-_{aq} \rightarrow O_2^{\bullet -} \qquad k = 2.3 \times 10^{10}\ M^{-1}\ s^{-1} \quad (23)$$

$$O_2 + H^{\bullet} \rightarrow HO_2^{\bullet} \qquad k = 1.3 \times 10^{10}\ M^{-1}\ s^{-1}, \quad (24)$$

where the superoxide anion radical $O_2^{\bullet -}$ is always in pH-dependent equilibrium with its conjugate radical, the hydroperoxyl radical $HO_2^{\bullet}$ [125]:

$$O_2^{\bullet -} + H^+ \leftrightarrow HO_2^{\bullet},\ pK_a(HO_2^{\bullet}/O_2^{\bullet -}) = 4.8 \text{ in water at } 25\ ^{\circ}C \quad (25)$$

Based on this pK_a, the Henderson–Hasselbalch equation indicates that $O_2^{\bullet -}$ is the predominant form of the hydroperoxyl radical in neutral water (pH 7). Using the reciprocal of the "scavenging power"—defined as the product of a solute's (or scavenger's) concentration and its rate constant for reaction with a primary radical species (units of s^{-1}) [5,13]—we can estimate the time scale over which O_2 scavenges e^-_{aq} or $H^{\bullet}$ atoms. In aerated water, these reactions occur within about 0.2–0.4 µs. This time scale roughly corresponds to the end of track expansion observed during low-LET irradiation (see supra).

In this context, the two-electron reduction product of oxygen, H_2O_2, can be generated through the dismutation reactions of the $HO_2^{\bullet}/O_2^{\bullet -}$ radicals as follows [125]:

$$HO_2^{\bullet} + HO_2^{\bullet} \rightarrow H_2O_2 + O_2, \qquad k = 8.3 \times 10^5\ M^{-1}\ s^{-1} \quad (26)$$

$$HO_2^{\bullet} + O_2^{\bullet -} + H^+ \rightarrow H_2O_2 + O_2, \qquad k = 9.7 \times 10^7\ M^{-1}\ s^{-1} \quad (27)$$

$$O_2^{\bullet -} + O_2^{\bullet -} + 2H^+ \rightarrow H_2O_2 + O_2, \qquad k = 0.3\ M^{-1}\ s^{-1}. \quad (28)$$

Given the rate of reaction (28), the reaction between two $O_2^{\bullet -}$ radicals in neutral aqueous solutions is negligible for all practical purposes. In living cells, superoxide dismutase (SOD) catalyzes this reaction, increasing the rate constant to ~4×10^9 M^{-1} s^{-1} at physiological pH [131–133]. This makes it one of the fastest enzyme-catalyzed reactions known, if not the fastest.

The presence of oxygen greatly influences the outcome of radiolysis, increasing the yield of oxidative products and creating a more oxidative, less reductive chemical environment. This is not only important for advancing our understanding of fundamental chemical processes but also holds broad practical significance. It is particularly relevant in diverse fields such as biology, radiobiology, radiation therapy, nuclear reactor chemistry, radioactive waste management, food preservation, and environmental chemistry, where radiolysis can affect the behavior and fate of pollutants. In addition, research on the radiolysis of aerated solutions has greatly enhanced our knowledge of both radical and bioradical oxygen chemistry (see, e.g., [11,53,132] and cited references).

2.3. Spurs/Tracks Are Highly Acidic

Experimental evidence [5,134,135] and Monte Carlo-based simulations [136–138] have demonstrated the occurrence of transient, highly acidic spikes immediately following water radiolysis. The underlying causes of this acidity are outlined below.

As described in Section 2.1, water molecules ionized into $H_2O^{\bullet +}$ dissociate within ~50 fs via the pseudo-first-order proton transfer reaction (1), producing H_3O^+ and $^\bullet$OH radicals close to the ionization site. Meanwhile, the secondary "dry" electron generated during ionization is ejected with several tens of electron-volts of kinetic energy, enabling it to travel an average distance of about 10 nm [139] before becoming thermalized and hydrated, a process that occurs within roughly one picosecond. At this stage, the hydrated electron, on the one hand, and H_3O^+ and the $^\bullet$OH radical, on the other hand, are quite far apart [140–142]. This spatial separation precludes immediate recombination through the following reactions [20]:

$$e^-_{aq} + H_3O^+ \rightarrow H^\bullet + H_2O, \qquad k = 2.1 \times 10^{10}\ M^{-1}\ s^{-1} \tag{29}$$

$$e^-_{aq} + {}^\bullet OH \rightarrow OH^-, \qquad k = 3.55 \times 10^{10}\ M^{-1}\ s^{-1}. \tag{30}$$

As a result, this initial charge separation generates a highly acidic environment surrounding the "native" radiation tracks. This acidity persists until the slow diffusion of H_3O^+ and $^\bullet$OH allows them to reach the distant location of e^-_{aq}, where reactions (29) and (30) eventually produce $H^\bullet$ and OH^-. This transient acid response, termed an "acid spike" [137], draws an analogy to the "thermal spike" sometimes used in radiation chemistry to describe a transient region of excess temperature formed around high-LET heavy ion tracks in water [54].

Figure 2a illustrates the temporal variations in H_3O^+ and OH^- yields from track chemistry simulations of low-LET radiolysis in pure, deaerated water at ambient temperature [116,137]. It also includes experimental data from ^{60}Co γ-ray or fast electron irradiation [143–147], demonstrating close agreement between simulated and measured yields of H_3O^+ and OH^-. Figure 2b displays the evolution of the corresponding pH, defined as $-\log[H_3O^+]$, where $[H_3O^+]$ represents the spur/track concentration of hydronium ions. For times shorter than ~1 ns, the pH remains stable at about 3.3 before gradually increasing to 7 (neutral water) at ~1 μs.

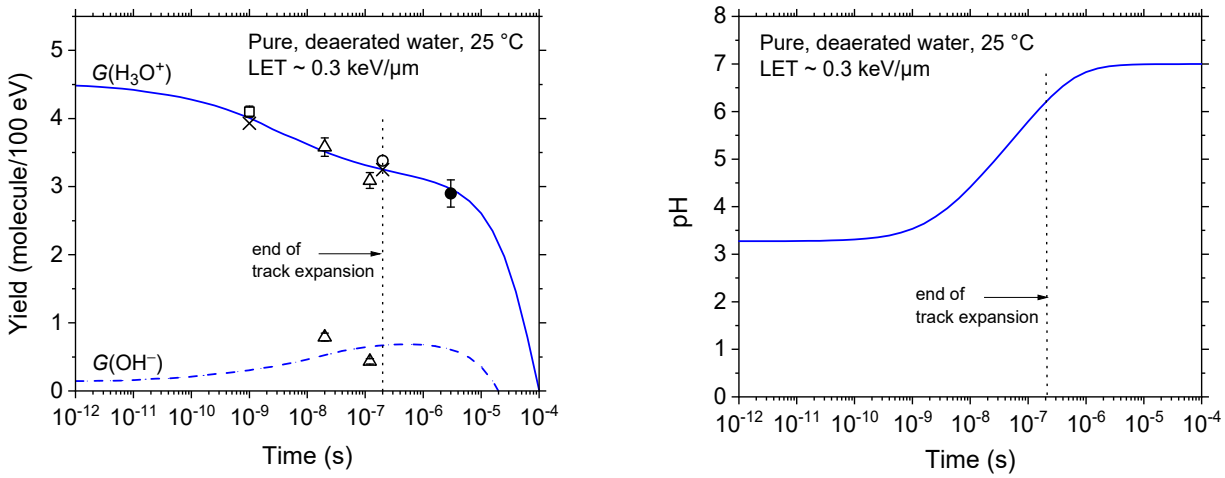

Figure 2. (**a**) Time evolution of the yields (in molecules per 100 eV) of radiolytically produced hydronium ions, $G(H_3O^+)$ (solid line), and hydroxide ions, $G(OH^-)$ (dashed line), derived from Monte Carlo simulations of the low-LET radiolysis of pure, deaerated water at 25 °C, over the range of ~1 ps to 100 μs [116,137]. Experimental data are shown as follows: (×) Čerček and Kongshaug [143], (○) Barker et al. [144], (□) Pikaev et al. [145], (Δ) Anderson et al. [146], and (•) Schmidt and Ander [147]. The thin vertical dotted line at ~0.2 μs marks the end of spur/track expansion, indicating the transition from nonhomogeneous track kinetics to homogeneous kinetics in the bulk solution; (**b**) Time-dependent pH variation calculated for pure, deaerated liquid water irradiated at 25 °C with low-LET radiation. Adapted from Bepari et al. [116] (Figure 2a) and Kanike et al. [137] (Figure 2b).

Although experiments and simulations confirm early acidity, acid-spike effects have been largely overlooked in studies of water exposed to ionizing radiation [148]. For example, from a radiation and free-radical biology perspective, this oversight is particularly surprising, given the high sensitivity of many biological structures and cellular processes to pH fluctuations [137,148–150].

2.4. LET and Dose-Rate Effects

Numerous experimental and theoretical studies have demonstrated that radiation quality, or equivalently, LET, significantly affects the yields of products in water radiolysis (see, e.g., [16,17,23,54] and references therein). As discussed in Section 2.1, low-LET radiation, often termed "sparsely" ionizing radiation, produces localized energy-loss events within small, nearly spherical volumes known as spurs. These spurs are spaced far enough apart to allow reactive species within them to engage in individual chemical pathways without significant interaction with neighboring spurs. In this scenario, the predominant effect of radiolysis is the formation of free radicals. In contrast, high-LET radiation, such as low-energy protons or heavy ions, neutrons, or α-particles, generates "densely" packed, continuous ionizing tracks of a cylindrical shape. This results in a concentrated and overlapping distribution of reactive species, fostering radical–radical interactions that enhance combination and recombination reactions within the diffusing tracks. Consequently, this reduces the yield of free radicals while promoting the formation of stable molecular entities like H_2, H_2O_2, and reformed water [5,53,54].

Under standard low- or high-LET irradiation conditions without dose-rate effects, radiation tracks do not overlap, which allows the chemical effects of irradiation to be considered as the sum of the effects of individual tracks, each evolving independently. However, increased radiation dose rates significantly alter the physicochemical and spatiotemporal dynamics due to overlapping radiation tracks, leading to enhanced inter-track chemistry (see, e.g., [5,53,116,136,151–153]). These intertrack radical–radical reactions in-

crease the proportion of molecular products at the expense of radical products (e^-_{aq}, $H^\bullet$, and $^\bullet OH$ radicals).

High dose rates and high LET values similarly affect radiolysis yields, despite their differing underlying mechanisms of action. Both conditions lead to increased radical densities, which favor radical–radical reactions either in the bulk of the solution (inter-track reactions) under high-dose-rate conditions or within individual radiation tracks (intra-track reactions) during high-LET irradiations.

3. The Ferrous Sulfate (Fricke) Dosimeter: The Most Thoroughly Studied System in Radiation Chemistry

3.1. The Primary Radical and Molecular Yields in Irradiated 0.4 M H_2SO_4 Aqueous Solutions

The vast majority of radiolysis experiments on acidic aqueous solutions were conducted starting in the 1950s, preceding those on neutral solutions (see, e.g., [121,129]). Sulfuric acid in 0.4 M aqueous solutions, with a pH of ~0.46, was the acid most commonly used [5,53]. This choice was primarily based on the understanding that the dominant anion, HSO_4^-, did not intervene in radiolysis processes under these conditions. Additionally, it is important to acknowledge the historical contributions of Hugo Fricke [154–157], who developed the ferrous sulfate dosimeter between 1927 and 1929. This dosimeter, a dilute solution of Fe^{2+} ions in 0.4 M H_2SO_4, was used in X-ray therapy. Fricke established that a 0.4 M sulfuric acid medium was necessary to match the response of the ferrous sulfate solution to that of air under X-ray exposure. Although using the 0.4 M sulfuric acid dosimeter offers no specific benefits in purely chemical studies, its continued use has largely been a matter of tradition [114].

The radical and molecular yields, derived from studies on a variety of mineral and organic systems in sulfuric acid environments, exhibit remarkable agreement [119], validating Allen's initial 1948 hypothesis of heterogeneous zones ("spurs") [158]. For all selected solutes within specific concentration limits, the generally accepted primary yields of radical and molecular products resulting from ^{60}Co γ-irradiation of 0.4 M H_2SO_4 aqueous solutions at 25 °C are [1,119,159]

$$\begin{array}{cccc} g(e^-_{aq}) = 0 & g(H^\bullet) = 3.70 & g(H_2) = 0.40 & \\ g(^\bullet OH) = 2.90 & g(H_2O_2) = 0.80 & g(HO_2^\bullet) = 0.02 & g(-H_2O) = 4.50, \end{array} \quad (31)$$

where the $HO_2^\bullet$ radical is produced in only very small yields and can generally be disregarded. These values also apply to hard X-rays and fast electrons of similar energies. Additionally, other acids, such as HCl, $HClO_4$ (perchloric acid), and $(COOH)_2$ (oxalic acid), have been utilized in determining radical and molecular yields at low pH (see [119] and references therein). A systematic review of the data indicates that the primary yield values in Equation (31) are generally consistent across solutions with the same pH, regardless of the anion type.

3.2. The Ferrous Sulfate, or Fricke, Dosimeter

In chemical dosimetry, the radiation dose is determined by the chemical changes occurring in a specific medium. Any well-characterized quantitative chemical reaction can serve as the basis for a dosimeter. The most thoroughly studied system in radiation chemistry is the air-saturated solution (~2.5×10^{-4} M O_2) of 1 mM ferrous sulfate in 0.4 M aqueous H_2SO_4, commonly known as the "Fricke dosimeter", named after Fricke [157]. Among all aqueous systems studied, this dosimeter stands out as the most widely used and best-understood chemical dosimeter. Its popularity stems from its accuracy, its reproducibility, and the linearity of its response to varying doses, making it essential in radiation-chemical research [5,160–162].

The chemistry of this system is based on the oxidation of ferrous ions to ferric ions by the oxidizing species $^{\bullet}OH$, $HO_2^{\bullet}$, and H_2O_2, which are generated during the radiolytic decomposition of water. The reaction scheme is as follows [5,129,157,163,164]:

$$e^-_{aq} + H_3O^+ \rightarrow H^{\bullet} + H_2O \qquad k = 2.1 \times 10^{10}\ M^{-1}\ s^{-1} \tag{29}$$

$$H^{\bullet} + O_2 \rightarrow HO_2^{\bullet} \qquad k = 1.3 \times 10^{10}\ M^{-1}\ s^{-1} \tag{24}$$

$$^{\bullet}OH + Fe^{2+} \rightarrow Fe^{3+} + OH^- \qquad k = 3.4 \times 10^{8}\ M^{-1}\ s^{-1} \tag{32}$$

$$HO_2^{\bullet} + Fe^{2+} \rightarrow Fe^{3+} + HO_2^- \qquad k = 7.9 \times 10^{5}\ M^{-1}\ s^{-1} \tag{33}$$

$$HO_2^- + H^+ \rightarrow H_2O_2 \qquad k = 5.0 \times 10^{10}\ M^{-1}\ s^{-1} \tag{34}$$

$$H_2O_2 + Fe^{2+} \rightarrow Fe^{3+} + {}^{\bullet}OH + OH^- \qquad k = 52\ M^{-1}\ s^{-1} \tag{35}$$

$$H^{\bullet} + Fe^{2+} + H^+ \rightarrow Fe^{3+} + H_2 \qquad k = 1.3 \times 10^{7}\ M^{-1}\ s^{-1}, \tag{36}$$

where the rate constants (k) provided here for the reactions between ions are at infinite dilution, corresponding to zero ionic strength. The yield of ferric ions is related to the primary radical and molecular yields given in Equation (31). In the presence of oxygen, the Fricke G-value, $G(Fe^{3+})$, is described by the following expression:

$$G(Fe^{3+})_{aerated} = g(^{\bullet}OH) + 3\,g(H^{\bullet}) + 2\,g(H_2O_2) + 3\,g(HO_2^{\bullet}). \tag{37}$$

Applying the yield values from Equation (31) results in a calculated $G(Fe^{3+})_{aerated}$ that falls well within 1–2% of the experimentally observed Fe^{3+} ion yield of 15.5 ± 0.2 ions/100 eV for ^{60}Co γ-rays or fast electrons [5,157,160–162,165].

In the absence of oxygen, reaction (24) is replaced by reaction (36), where $H^{\bullet}$ assumes the atypical role of an oxidizing agent, oxidizing one Fe^{2+} ion—compared to three in an aerated solution. Under these conditions, the Fricke G-value becomes

$$G(Fe^{3+})_{deaerated} = g(^{\bullet}OH) + g(H^{\bullet}) + 2\,g(H_2O_2) + 3\,g(HO_2^{\bullet}), \tag{38}$$

where the experimentally observed $G(Fe^{3+})_{deaerated}$ value is 8.2 ± 0.3 ions/100 eV for ^{60}Co γ-radiation [5,129,157,165].

In normally air-saturated solutions, oxygen is consumed during irradiation, causing the $G(Fe^{3+})$ value to fall from 15.5 to 8.2 ions/100 eV once the oxygen is depleted. This oxygen consumption imposes an upper usage limit of about 400 Gy for the "standard" Fricke dosimeter. However, the system can be adjusted to extend the dosimeter's capacity to measure higher radiation doses (up to 2000 Gy) by using an oxygen-saturated solution (~1.3×10^{-3} M O_2) and increasing the Fe^{2+} concentration to 10 mM, thereby forming what is known as the "super" Fricke dosimeter. Under these conditions, the accepted value of the Fricke yield is 16.1 ions/100 eV for low-LET radiation within the limit of low dose rates [166].

The kinetics of Fe^{3+} formation in the Fricke dosimeter have been extensively detailed (see, e.g., [163,164,167–169] and references therein). $G(Fe^{3+})$ is time-dependent, reflecting differences in the time scales of the reactions of Fe^{2+} with the species produced by the radiolysis of acidic water under aerated or deaerated conditions, as described by reactions (32), (33), (35), and (36). For instance, the fastest Fe^{3+} formation occurs through Fe^{2+} oxidation by $^{\bullet}OH$ radicals, while the slowest arises from its reaction with H_2O_2. To illustrate, Figure 3a,b present the time evolution of $G(Fe^{3+})$ obtained from Monte Carlo simulations of the low-LET radiolysis of the Fricke dosimeter under aerated and deaerated conditions, respectively, at 25 °C, over the interval of ~1 ps–200 s, without dose-rate effects [168,169].

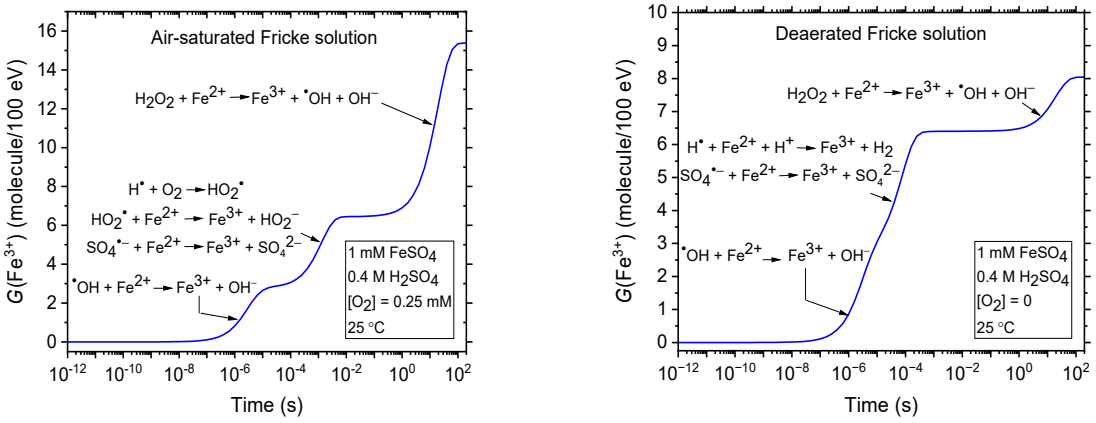

Figure 3. Temporal evolution of $G(Fe^{3+})$ obtained through Monte Carlo simulations of low-LET radiolysis of the Fricke solution under aerated (**a**) and deaerated (**b**) conditions at 25 °C, over the interval of ~1 ps–200 s [168,169]. For solutions containing 0.4 M H_2SO_4, a small number of $^{\bullet}OH$ radicals react with HSO_4^-, forming sulfate radicals, $SO_4^{\bullet-}$. Despite this, the overall Fe^{3+} yield remains consistent with Equations (37) and (38), as $SO_4^{\bullet-}$ reacts with Fe^{2+} similarly to $^{\bullet}OH$ [163], the reaction being represented as $SO_4^{\bullet-} + Fe^{2+} \rightarrow Fe^{3+} + SO_4^{2-}$, with a rate constant $k = 9.9 \times 10^8$ M^{-1} s^{-1}. Adapted from Penabeï et al. [169].

Finally, Equations (37) and (38) demonstrate that Fe^{3+} ion formation is highly sensitive to factors affecting the primary free-radical yields ($H^{\bullet}$, $^{\bullet}OH$, and $HO_2^{\bullet}$), such as LET and dose rate. As previously mentioned, raising the LET or dose rate promotes intra- or inter-track radical–radical reactions that compete with the radicals' reactions with Fe^{2+}, ultimately reducing $G(Fe^{3+})$ [139,151]. This effect is illustrated in Figure 4a,b.

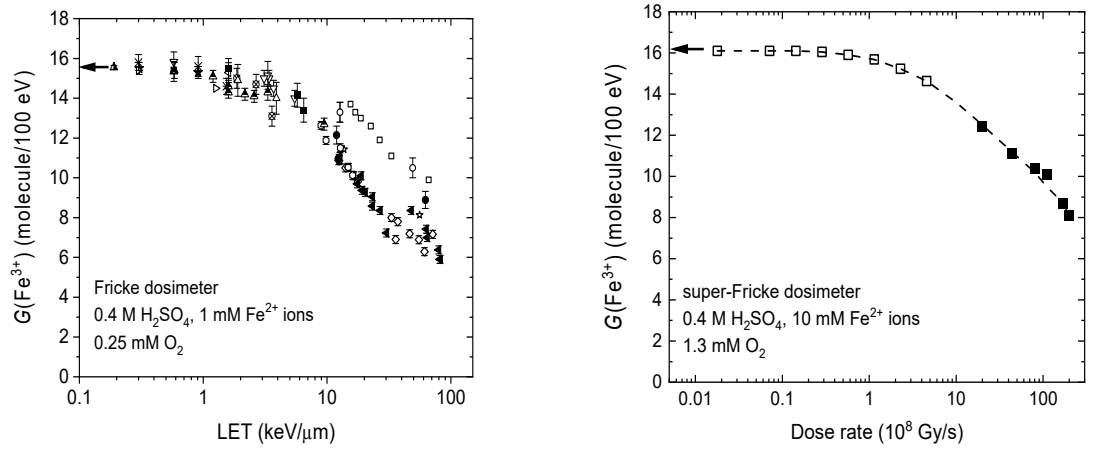

Figure 4. (**a**) A plot showing the ferric ion yield, $G(Fe^{3+})$, from the radiolysis of the aerated Fricke solution at 25 °C against LET over the range of ~0.3–70 keV/µm. The symbols represent experimental data gathered from various radiation sources and energies, compiled from multiple studies. Detailed references are provided in [164,168]. The arrow on the left of the figure indicates the accepted yield value of 15.5 molecules per 100 eV for the air-saturated Fricke dosimeter for ^{60}Co γ-rays or fast electrons. Adapted from Tippayamontri et al. [164]. (**b**) Experimental data of $G(Fe^{3+})$ for the super-Fricke dosimeter. Open squares correspond to data from Sehested et al. [166] (see also [162] and [170]). Filled squares correspond to data from Trupin-Wasselin [171]. The arrow on the left of the figure indicates the accepted yield value of 16.1 molecules per 100 eV for the super-Fricke dosimeter under ^{60}Co γ-ray or fast electron irradiation in the absence of dose-rate effects. Dose rates are expressed in Gy/s. Adapted with permission from Alanazi et al. [153]. © 2025 Radiation Research Society.

4. Conclusions

This short review of the fundamentals of water radiolysis underscores the importance of a thorough understanding of its mechanisms and outcomes for managing chemical processes in radiation-exposed aqueous environments. This, in turn, emphasizes the ongoing need for both experimental and theoretical studies to further advance knowledge in this critical field.

In an upcoming article, we aim to present a comprehensive review of water radiolysis, focusing on its temperature dependence and behavior in the sub- and supercritical regimes. Special attention will be given to its implications for water chemistry in nuclear reactors, highlighting key mechanisms, experimental findings, and their relevance to reactor operation and safety.

Funding: This research was funded by the Natural Sciences and Engineering Research Council of Canada (NSERC), grant number RGPIN-2022-03972.

Institutional Review Board Statement: Not applicable.

Informed Consent Statement: Not applicable.

Data Availability Statement: All data generated or analyzed during this study are provided in full within the article. For further inquiries, please contact the author directly.

Acknowledgments: This work is dedicated to the memory of Professor Christiane Ferradini, who introduced me to the fascinating field of water radiation chemistry. Our close collaboration, from the summer of 1987 until her passing in May 2002, spanned both the Université René Descartes in Paris and the Université de Sherbrooke in Canada. As an exceptional mentor, her wisdom and unwavering encouragement profoundly influenced the course of my research and inspired many young scholars under my supervision at the Université de Sherbrooke, hailing from diverse locations worldwide, including Thailand, Japan, Bangladesh, Morocco, India, Indonesia, Colombia, Chad, Iran, Cameroon, and Saudi Arabia. Her enduring legacy continues to guide my ongoing endeavors in this field.

Conflicts of Interest: The author declares no conflicts of interest.

References

1. Ferradini, C.; Pucheault, J. *Biologie de l'Action des Rayonnements Ionisants*; Masson: Paris, France, 1983.
2. Buxton, G.V. Radiation chemistry of the liquid state: (1) Water and homogeneous aqueous solutions. In *Radiation Chemistry: Principles and Applications*; Farhataziz, Rodgers, M.A.J., Eds.; VCH: New York, NY, USA, 1987; pp. 321–349.
3. Freeman, G.R. (Ed.) *Kinetics of Nonhomogeneous Processes: A Practical Introduction for Chemists, Biologists, Physicists, and Materials Scientists*; Wiley: New York, NY, USA, 1987.
4. Magee, J.L. Nonhomogeneous processes in radiation research: Radical diffusion models. *Can. J. Phys.* **1990**, *68*, 853–857. [CrossRef]
5. Spinks, J.W.T.; Woods, R.J. *An Introduction to Radiation Chemistry*, 3rd ed.; Wiley: New York, NY, USA, 1990.
6. Tabata, Y.; Ito, Y.; Tagawa, S. (Eds.) *CRC Handbook of Radiation Chemistry*; CRC Press: Boca Raton, FL, USA, 1991.
7. Klassen, N.V. Primary species in irradiated water. *J. Chim. Phys.* **1991**, *88*, 747–757. [CrossRef]
8. Ferradini, C.; Jay-Gerin, J.-P. (Eds.) *Excess Electrons in Dielectric Media*; CRC Press: Boca Raton, FL, USA, 1991.
9. Draganić, I.G.; Draganić, Z.D.; Adloff, J.-P. *Radiation and Radioactivity on Earth and Beyond*, 2nd ed.; CRC Press: Boca Raton, FL, USA, 1993. [CrossRef]
10. Bensasson, R.V.; Land, E.J.; Truscott, T.G. *Excited States and Free Radicals in Biology and Medicine*; Oxford University Press: Oxford, UK, 1993.
11. Woods, R.J.; Pikaev, A.K. *Applied Radiation Chemistry: Radiation Processing*; Wiley: New York, NY, USA, 1994.
12. Getoff, N. Radiation-induced degradation of water pollutants—State of the art. *Radiat. Phys. Chem.* **1996**, *47*, 581–593. [CrossRef]
13. McCracken, D.R.; Tsang, K.T.; Laughton, P.J. *Aspects of the Physics and Chemistry of Water Radiolysis by Fast Neutrons and Fast Electrons in Nuclear Reactors*; Report AECL-11895; Atomic Energy of Canada Limited: Chalk River, ON, Canada, 1998.
14. Richter, H.W. Radiation chemistry: Principles and applications. In *Photochemistry and Radiation Chemistry. Complementary Methods for the Study of Electron Transfer*; Wishart, J.F., Nocera, D.G., Eds.; American Chemical Society: Washington, DC, USA, 1998; Chapter 2; pp. 5–33. [CrossRef]

15. Pastina, B.; LaVerne, J.A.; Pimblott, S.M. Dependence of molecular hydrogen formation in water on scavengers of the precursor to the hydrated electron. *J. Phys. Chem. A* **1999**, *103*, 5841–5846. [CrossRef]
16. Mozumder, A. *Fundamentals of Radiation Chemistry*; Academic Press: San Diego, CA, USA, 1999.
17. LaVerne, J.A. Radiation chemical effects of heavy ions. In *Charged Particle and Photon Interactions with Matter: Chemical, Physicochemical, and Biological Consequences with Applications*; Mozumder, A., Hatano, Y., Eds.; Marcel Dekker: New York, NY, USA, 2004; pp. 403–429.
18. Garrett, B.C.; Dixon, D.A.; Camaioni, D.M.; Chipman, D.M.; Johnson, M.A.; Jonah, C.D.; Kimmel, G.A.; Miller, J.H.; Rescigno, T.N.; Rossky, P.J.; et al. Role of water in electron-initiated processes and radical chemistry: Issues and scientific advances. *Chem. Rev.* **2005**, *105*, 355–389. [CrossRef]
19. von Sonntag, C. *Free-Radical-Induced DNA Damage and Its Repair. A Chemical Perspective*; Springer: Berlin, Germany, 2006.
20. Elliot, A.J.; Bartels, D.M. *The Reaction Set, Rate Constants and g-Values for the Simulation of the Radiolysis of Light Water over the Range 20 to 350 °C Based on Information Available in 2008*; Report No. 153-127160-450-001; Atomic Energy of Canada Limited: Mississauga, ON, Canada, 2009.
21. Lin, M.; Muroya, Y.; Baldacchino, G.; Katsumura, Y. Radiolysis of supercritical water. In *Recent Trends in Radiation Chemistry*; Wishart, J.F., Rao, B.S.M., Eds.; World Scientific: Hackensack, NJ, USA, 2010; pp. 255–277.
22. Muroya, Y.; Lin, M.; de Waele, V.; Hatano, Y.; Katsumura, Y.; Mostafavi, M. First observation of picosecond kinetics of hydrated electrons in supercritical water. *J. Phys. Chem. Lett.* **2010**, *1*, 331–335. [CrossRef]
23. Meesungnoen, J.; Jay-Gerin, J.-P. Radiation chemistry of liquid water with heavy ions: Monte Carlo simulation studies. In *Charged Particle and Photon Interactions with Matter. Recent Advances, Applications, and Interfaces*; Hatano, Y., Katsumura, Y., Mozumder, A., Eds.; CRC Press (Taylor & Francis Group): Boca Raton, FL, USA, 2011; pp. 355–400. [CrossRef]
24. Bobrowski, K. Radiation-induced radical reactions. In *Encyclopedia of Radicals in Chemistry, Biology and Materials*; Chatgilialoglu, C., Studer, A., Eds.; Wiley: Chichester, UK, 2012; Volume 1, pp. 395–432. [CrossRef]
25. Das, S. Critical review of water radiolysis processes, dissociation products, and possible impacts on the local environment: A geochemist's perspective. *Aust. J. Chem.* **2013**, *66*, 522–529. [CrossRef]
26. Wojnárovits, L.; Takács, E. Radiation induced degradation of organic pollutants in waters and wastewaters. *Top. Curr. Chem. (Z)* **2016**, *374*, 50. [CrossRef]
27. Katsumura, Y.; Kudo, H. Radiation chemistry of aqueous solutions. In *Radiation Applications*; Kudo, H., Ed.; Springer Nature: Singapore, 2018; Chapter 6; pp. 37–49. [CrossRef]
28. Wardman, P. Radiotherapy using high-intensity pulsed radiation beams (FLASH): A radiation-chemical perspective. *Radiat. Res.* **2020**, *194*, 607–617. [CrossRef] [PubMed]
29. Macdonald, D.D.; Engelhardt, G.R.; Petrov, A. A critical review of radiolysis issues in water-cooled fission and fusion reactors: Part I, Assessment of radiolysis models. *Corros. Mater. Degrad.* **2022**, *3*, 470–535. [CrossRef]
30. Fritsch, B.; Lee, S.; Körner, A.; Schneider, N.M.; Ross, F.M.; Hutzler, A. The influence of ionizing radiation on quantification for in situ and operando liquid-phase electron microscopy. *Adv. Mater.* **2025**, 2415728. [CrossRef] [PubMed]
31. Medin, J.; Ross, C.K.; Klassen, N.V.; Palmans, H.; Grusell, E.; Grindborg, J.-E. Experimental determination of beam quality factors, k_Q, for two types of Farmer chamber in a 10 MV photon and a 175 MeV proton beam. *Phys. Med. Biol.* **2006**, *51*, 1503–1521. [CrossRef] [PubMed]
32. Curie, P.; Curie, S. Sur une substance nouvelle radio-active, contenue dans la pechblende. *C. R. Acad. Sci. Paris* **1898**, *127*, 175–178.
33. Curie, P.; Curie, P. (Mme); Bémont, G. Sur une nouvelle substance fortement radio-active, contenue dans la pechblende. *C. R. Acad. Sci. Paris* **1898**, *127*, 1215–1217.
34. Curie, P.; Debierne, A. Sur la radio-activité induite et les gaz activés par le radium. *C. R. Acad. Sci. Paris* **1901**, *132*, 768–770.
35. Giesel, F. Ueber Radium und radioactive Stoffe. *Ber. Deutsch. Chem. Ges. (Berlin)* **1902**, *35*, 3608–3611. [CrossRef]
36. Giesel, F. Ueber den Emanationskörper aus Pechblende und über Radium. *Ber. Deutsch. Chem. Ges.* **1903**, *36*, 342–347. [CrossRef]
37. Ramsey, W.; Soddy, F. Experiments in radioactivity, and the production of helium from radium. *Proc. R. Soc. London* **1903**, *72*, 204–207.
38. Curie, P. *Radioactivité*; Hermann: Paris, France, 1935; p. 347.
39. Rutherford, E.; Royds, T. The nature of the α particle from radioactive substances. *Philos. Mag.* **1909**, *17*, 281–286. [CrossRef]
40. Ramsey, W. The chemical action of the radium emanation. Part I. Action on distilled water. *J. Chem. Soc. Trans.* **1907**, *91*, 931–942. [CrossRef]
41. Cameron, A.T.; Ramsey, W. The chemical action of radium emanation. Part II. On solutions containing copper, and lead, and on water. *J. Chem. Soc. Trans.* **1907**, *91*, 1593–1606. [CrossRef]
42. Usher, F.L. Die chemische Einzelwirkung und die chemische Gesamtwirkung der α- und der β-Strahlen. *Jahrb. Radioakt. Elektr.* **1911**, *8*, 323–334.
43. Kernbaum, M. Action chimique sur l'eau des rayons pénétrants de radium. *C. R. Acad. Sci. Paris* **1909**, *148*, 705–706.
44. Risse, O. Über die Röntgenphotolyse des Hydroperoxyds. *Z. Phys. Chem.* **1929**, *140A*, 133–157. [CrossRef]

45. Fricke, H.; Brownscombe, E.R. Inability of X-rays to decompose water. *Phys. Rev.* **1933**, *44*, 240. [CrossRef]
46. Debierne, A. Recherches sur les gaz produits par les substances radioactives. Décomposition de l'eau. *Ann. Physique (Paris)* **1914**, *2*, 97–127. [CrossRef]
47. Risse, O. Einige Bemerkungen zum Mechanismus chemischer Röntgenreaktionen in wäβrigen Lösungen. *Strahlentherapie* **1929**, *34*, 578–581.
48. Allen, A.O. Mechanism of the radiolysis of water by gamma rays or electrons. In *Actions Chimiques et Biologiques des Radiations*; Haïssinsky, M., Ed.; Masson: Paris, France, 1961; Volume 5, pp. 9–30.
49. Gordon, S. Radiation chemistry at the Metallurgical Laboratory, Manhattan project, University of Chicago (1942–1947) and the Argonne National Laboratory, Argonne, IL (1947–1984). In *Early Developments in Radiation Chemistry*; Kroh, J., Ed.; The Royal Society of Chemistry, Thomas Graham House: Cambridge, UK, 1989; pp. 163–204.
50. Weiss, J. Radiochemistry of aqueous solutions. *Nature* **1944**, *153*, 748–750. [CrossRef]
51. Kroh, J. (Ed.) *Early Developments in Radiation Chemistry*; The Royal Society of Chemistry, Thomas Graham House: Cambridge, UK, 1989.
52. Jonah, C.D. A short history of the radiation chemistry of water. *Radiat. Res.* **1995**, *144*, 141–147. [CrossRef]
53. Ferradini, C.; Jay-Gerin, J.-P. Radiolysis of water and aqueous solutions: History and present state of the science. *Can. J. Chem.* **1999**, *77*, 1542–1575. [CrossRef]
54. LaVerne, J.A. Track effects of heavy ions in liquid water. *Radiat. Res.* **2000**, *153*, 487–496. [CrossRef] [PubMed]
55. Zimbrick, J.D. Radiation chemistry and the Radiation Research Society: A history from the beginning. *Radiat. Res.* **2002**, *158*, 127–140. [CrossRef]
56. Buxton, G.V. The radiation chemistry of liquid water: Principles and Applications. In *Charged Particle and Photon Interactions with Matter: Chemical, Physicochemical, and Biological Consequences with Applications*; Mozumder, A., Hatano, Y., Eds.; Marcel Dekker: New York, NY, USA, 2004; pp. 331–363.
57. Cooper, R. The history and development of radiation chemistry. *Aust. J. Chem.* **2011**, *64*, 864–868. [CrossRef]
58. Le Caër, S. Water radiolysis: Influence of oxide surfaces on H_2 production under ionizing radiation. *Water* **2011**, *3*, 235–253. [CrossRef]
59. Baldacchino, G. The contribution of swift ions in the epic of radiation chemistry. *Histoire de la Recherche Contemporaine* **2017**, *Tome VI*, 47–54. [CrossRef]
60. Zimbrick, J.D. Radiation chemistry and Radiation Research: A history from the beginning to the Platinum edition. *Radiat. Res.* **2024**, *202*, 368–384. [CrossRef]
61. Platzman, R.L. The physical and chemical basis of mechanisms in radiation biology. In *Radiation Biology and Medicine. Selected Reviews in the Life Sciences*; Claus, W.D., Ed.; Addison-Wesley: Reading, MA, USA, 1958; pp. 15–72.
62. Kuppermann, A. Theoretical foundations of radiation chemistry. *J. Chem. Educ.* **1959**, *36*, 279–285. [CrossRef]
63. Loh, Z.-H.; Doumy, G.; Arnold, C.; Kjellsson, L.; Southworth, S.H.; Al Haddad, A.; Kumagai, Y.; Tu, M.-F.; Ho, P.J.; March, A.M.; et al. Observation of the fastest chemical processes in the radiolysis of water. *Science* **2020**, *367*, 179–182. [CrossRef]
64. Ogura, H.; Hamill, W.H. Positive hole migration in pulse-irradiated water and heavy water. *J. Phys. Chem.* **1973**, *77*, 2952–2954. [CrossRef]
65. Cobut, V.; Frongillo, Y.; Patau, J.P.; Goulet, T.; Fraser, M.-J.; Jay-Gerin, J.-P. Monte Carlo simulation of fast electron and proton tracks in liquid water—I. Physical and physicochemical aspects. *Radiat. Phys. Chem.* **1998**, *51*, 229–243. [CrossRef]
66. Cobut, V.; Frongillo, Y.; Jay-Gerin, J.-P.; Patau, J.P. A Monte Carlo calculation of subexcitation and vibrationally-relaxing electron spectra in irradiated liquid water. *Radiat. Phys. Chem.* **1992**, *40*, 589–591. [CrossRef]
67. LaVerne, J.A.; Pimblott, S.M. Electron energy-loss distributions in solid, dry DNA. *Radiat. Res.* **1995**, *141*, 208–215. [CrossRef]
68. Autsavapromporn, N. The Effects of pH and Radiation Quality (LET) on the Radiolysis of Liquid Water and Aqueous Solutions: A Monte Carlo Simulation Study. Master's Thesis, Burapha University, Chonburi, Thailand, 2006.
69. Michaud, M.; Cloutier, P.; Sanche, L. Low-energy electron-energy-loss spectroscopy of amorphous ice: Electronic excitations. *Phys. Rev. A* **1991**, *44*, 5624–5627. [CrossRef] [PubMed]
70. Goulet, T.; Bernas, A.; Ferradini, C.; Jay-Gerin, J.-P. On the electronic structure of liquid water: Conduction-band tail revealed by photoionization data. *Chem. Phys. Lett.* **1990**, *170*, 492–496. [CrossRef]
71. Migus, A.; Gauduel, Y.; Martin, J.L.; Antonetti, A. Excess electrons in liquid water: First evidence of a prehydrated state with femtosecond lifetime. *Phys. Rev. Lett.* **1987**, *58*, 1559–1562. [CrossRef]
72. Pépin, C.; Goulet, T.; Houde, D.; Jay-Gerin, J.-P. Observation of a continuous spectral shift in the solvation kinetics of electrons in neat liquid deuterated water. *J. Phys. Chem. A* **1997**, *101*, 4351–4360. [CrossRef]
73. LaForge, A.C.; Michiels, R.; Bohlen, M.; Callegari, C.; Clark, A.; von Conta, A.; Coreno, M.; Di Fraia, M.; Drabbels, M.; Huppert, M.; et al. Real-time dynamics of the formation of hydrated electrons upon irradiation of water clusters with extreme ultraviolet light. *Phys. Rev. Lett.* **2019**, *122*, 133001. [CrossRef]

74. Sopena Moros, A.; Li, S.; Li, K.; Doumy, G.; Southworth, S.H.; Otolski, C.; Schaller, R.D.; Kumagai, Y.; Rubensson, J.-E.; Simon, M.; et al. Tracking cavity formation in electron solvation: Insights from X-ray spectroscopy and theory. *J. Am. Chem. Soc.* **2024**, *146*, 3262–3269. [CrossRef]
75. Klassen, N.V. Primary products in radiation chemistry. In *Radiation Chemistry: Principles and Applications*; Farhataziz, Rodgers, M.A.J., Eds.; VCH Publishers: New York, NY, USA, 1987; pp. 29–64.
76. Bernas, A.; Ferradini, C.; Jay-Gerin, J.-P. Excess electrons in homogeneous and heterogeneous polar media. *Can. J. Chem.* **1996**, *74*, 1–23. [CrossRef]
77. Yamamoto, Y.-I.; Suzuki, T. Ultrafast dynamics of water radiolysis: Hydrated electron formation, solvation, recombination, and scavenging. *J. Phys. Chem. Lett.* **2020**, *11*, 5510–5516. [CrossRef]
78. Platzman, R.L. Dissociative attachment of subexcitation electrons in liquid water, and the origin of radiolytic "molecular" hydrogen. In *Book of Abstracts, Proceedings of the 2nd International Congress of Radiation Research (ICRR), Harrogate, UK, 5–11 August 1962*; The University of Chicago: Chicago, IL, USA; p. 128.
79. Rowntree, P.; Parenteau, L.; Sanche, L. Electron stimulated desorption via dissociative attachment in amorphous H_2O. *J. Chem. Phys.* **1991**, *94*, 8570–8576. [CrossRef]
80. Goulet, T.; Patau, J.P.; Jay-Gerin, J.-P. Influence of the parent cation on the thermalization of subexcitation electrons in solid water. *J. Phys. Chem.* **1990**, *94*, 7312–7316. [CrossRef]
81. Swiatla-Wojcik, D.; Buxton, G.V. Modeling of radiation spur processes in water at temperatures up to 300 °C. *J. Phys. Chem.* **1995**, *99*, 11464–11471. [CrossRef]
82. Taube, H. Photochemical reactions of ozone in solution. *Trans. Faraday Soc.* **1957**, *53*, 656–665. [CrossRef]
83. Biedenkapp, D.; Hartshorn, L.G.; Bair, E.J. The $O(^1D)$ + H_2O reaction. *Chem. Phys. Lett.* **1970**, *5*, 379–381. [CrossRef]
84. Amichai, O.; Treinin, A. Chemical reactivity of $O(^3P)$ atoms in aqueous solution. *Chem. Phys. Lett.* **1969**, *3*, 611–613. [CrossRef]
85. Nikogosyan, D.N.; Oraevsky, A.A.; Rupasov, V.I. Two-photon ionization and dissociation of liquid water by powerful laser UV radiation. *Chem. Phys.* **1983**, *77*, 131–143. [CrossRef]
86. Crowell, R.A.; Bartels, D.M. Multiphoton ionization of liquid water with 3.0–5.0 eV photons. *J. Phys. Chem.* **1996**, *100*, 17940–17949. [CrossRef]
87. Bernas, A.; Ferradini, C.; Jay-Gerin, J.-P. On the electronic structure of liquid water: Facts and reflections. *Chem. Phys.* **1997**, *222*, 151–160. [CrossRef]
88. Faraggi, M. On the molecular hydrogen formation in the gamma radiolysis of water and aqueous solutions. *Int. J. Radiat. Phys. Chem.* **1973**, *5*, 197–206. [CrossRef]
89. Cobut, V.; Jay-Gerin, J.-P.; Frongillo, Y.; Patau, J.P. On the dissociative electron attachment as a potential source of molecular hydrogen in irradiated liquid water. *Radiat. Phys. Chem.* **1996**, *47*, 247–250. [CrossRef]
90. Sanguanmith, S. Breaking the Picosecond Barrier in the Physics and Chemistry of Water Radiolysis: Applications of Monte Carlo Modeling to High-Temperature Nuclear Reactors and Radiobiology. Ph.D. Thesis, Université de Sherbrooke, Sherbrooke, QC, Canada, 2021.
91. LaVerne, J.A.; Pimblott, S.M. New mechanism for H_2 formation in water. *J. Phys. Chem. A* **2000**, *104*, 9820–9822. [CrossRef]
92. Harris, R.E.; Pimblott, S.M. On ^3H β-particle and ^{60}Co γ irradiation of aqueous systems. *Radiat. Res.* **2002**, *158*, 493–504. [CrossRef]
93. Horne, G.P.; Pimblott, S.M.; LaVerne, J.A. Inhibition of radiolytic molecular hydrogen formation by quenching of excited state water. *J. Phys. Chem. B* **2017**, *121*, 5385–5390. [CrossRef] [PubMed]
94. Schwarz, H.A. Applications of the spur diffusion model to the radiation chemistry of aqueous solutions. *J. Phys. Chem.* **1969**, *73*, 1928–1937. [CrossRef]
95. Dobrovolskii, D.; Denisov, S.A.; Sims, H.E.; Mostafavi, M. Reactivity of quasi-free electrons towards N_3^- and its impact on H_2 formation mechanism in water radiolysis. *Phys. Chem. Chem. Phys.* **2024**, *26*, 11604–11610. [CrossRef]
96. Sims, H.E. (Central Laboratory, National Nuclear Laboratory, Sellafield, Seascale, UK). Personal communication, 2024.
97. Hunt, J.W. Early events in radiation chemistry. In *Advances in Radiation Chemistry*; Burton, M., Magee, J.L., Eds.; Wiley: New York, NY, USA, 1976; Volume 5, pp. 185–315.
98. Jonah, C.D.; Miller, J.R.; Matheson, M.S. The reaction of the precursor of the hydrated electron with electron scavengers. *J. Phys. Chem.* **1977**, *81*, 1618–1622. [CrossRef]
99. Pimblott, S.M.; LaVerne, J.A. On the radiation chemical kinetics of the precursor to the hydrated electron. *J. Phys. Chem. A* **1998**, *102*, 2967–2975. [CrossRef]
100. Lu, Q.-B.; Baskin, J.S.; Zewail, A.H. The presolvated electron in water: Can it be scavenged at long range? *J. Phys. Chem. B* **2004**, *108*, 10509–10514. [CrossRef]
101. Ma, J.; Wang, F.; Denisov, S.A.; Adhikary, A.; Mostafavi, M. Reactivity of prehydrated electrons toward nucleobases and nucleotides in aqueous solution. *Sci. Adv.* **2017**, *3*, e1701669. [CrossRef]
102. Ferradini, C.; Jay-Gerin, J.-P. Hypothesis of a possible chemical fate for the incompletely relaxed electron in water and alcohols. *Chem. Phys. Lett.* **1990**, *167*, 371–373. [CrossRef]

103. Ferradini, C.; Jay-Gerin, J.-P. Does multiple ionization intervene for the production of $HO_2^{\bullet}$ radicals in high-LET liquid water radiolysis? *Radiat. Phys. Chem.* **1998**, *51*, 263–267. [CrossRef]
104. Ferradini, C. Actions chimiques des radiations ionisantes. *J. Chim. Phys.* **1979**, *76*, 636–644. [CrossRef]
105. Chatterjee, A.; Holley, W.R. Computer simulation of initial events in the biochemical mechanisms of DNA damage. *Adv. Radiat. Biol.* **1993**, *17*, 181–221. [CrossRef] [PubMed]
106. Muroya, Y.; Plante, I.; Azzam, E.I.; Meesungnoen, J.; Katsumura, Y.; Jay-Gerin, J.-P. High-LET ion radiolysis of water: Visualization of the formation and evolution of ion tracks and relevance to the radiation-induced bystander effect. *Radiat. Res.* **2006**, *165*, 485–491. [CrossRef] [PubMed]
107. International Commission on Radiation Units and Measurements. *Linear Energy Transfer*; ICRU Report No. 16; International Commission on Radiation Units and Measurements: Washington, DC, USA, 1970.
108. Magee, J.L. Radiation chemistry. *Annu. Rev. Nucl. Sci.* **1953**, *3*, 171–192. [CrossRef]
109. Freeman, G.R. Basics of radiation chemistry. In *The Study of Fast Processes and Transient Species by Electron Pulse Radiolysis*; Baxendale, J.H., Busi, F., Eds.; Reidel Publishing: Dordrecht, The Netherlands, 1982; pp. 19–34.
110. Plante, I.L.; Filali-Mouhim, A.; Jay-Gerin, J.-P. SIMULRAD: A JAVA interface for a Monte Carlo simulation code to visualize in 3D the early stages of water radiolysis. *Radiat. Phys. Chem.* **2005**, *72*, 173–180. [CrossRef]
111. Sanguanmith, S.; Meesungnoen, J.; Muroya, Y.; Lin, M.; Katsumura, Y.; Jay-Gerin, J.-P. On the spur lifetime and its temperature dependence in the low linear energy transfer radiolysis of water. *Phys. Chem. Chem. Phys.* **2012**, *14*, 16731–16736. [CrossRef]
112. Kuppermann, A.; Belford, G.G. Diffusion kinetics in radiation chemistry. I. Generalized formulation and criticism of diffusion model. *J. Chem. Phys.* **1962**, *36*, 1412–1426. [CrossRef]
113. Dewhurst, H.A.; Burton, M. Radiolysis of aqueous solutions of hydrazine. *J. Am. Chem. Soc.* **1955**, *77*, 5781–5785. [CrossRef]
114. Hart, E.J. Chemical effects of ionizing radiations on aqueous inorganic solutions. *J. Chem. Educ.* **1957**, *34*, 586–593. [CrossRef]
115. Pastina, B.; LaVerne, J.A. Effect of molecular hydrogen on hydrogen peroxide in water radiolysis. *J. Phys. Chem. A* **2001**, *105*, 9316–9322. [CrossRef]
116. Bepari, M.I.; Meesungnoen, J.; Jay-Gerin, J.-P. Early and transient formation of highly acidic pH spikes in water radiolysis under the combined effect of high dose rate and high linear energy transfer. *Radiation* **2023**, *3*, 165–182. [CrossRef]
117. Schwarz, H.A. Reaction of the hydrated electron with water. *J. Phys. Chem.* **1992**, *96*, 8937–8941. [CrossRef]
118. Elliot, A.J.; Chenier, M.P.; Ouellette, D.C. Temperature dependence of g values for H_2O and D_2O irradiated with low linear energy transfer radiation. *J. Chem. Soc. Faraday Trans.* **1993**, *89*, 1193–1197. [CrossRef]
119. Ferradini, C.; Jay-Gerin, J.-P. The effect of pH on water radiolysis: A still open question—A minireview. *Res. Chem. Intermed.* **2000**, *26*, 549–565. [CrossRef]
120. Buxton, G.V. An overview of the radiation chemistry of liquids. In *Radiation Chemistry: From Basics to Applications in Material and Life Sciences*; Spotheim-Maurizot, M., Mostafavi, M., Douki, T., Belloni, J., Eds.; EDP Sciences: Les Ulis, France, 2008; pp. 3–16. [CrossRef]
121. Draganić, I.G.; Draganić, Z.D. *The Radiation Chemistry of Water*; Academic Press: New York, NY, USA, 1971.
122. Draganić, I.G.; Nenadović, M.T.; Draganić, Z.D. Radiolysis of HCOOH + O_2 at pH 1.3–13 and the yields of primary products in γ radiolysis of water. *J. Phys. Chem.* **1969**, *73*, 2564–2571. [CrossRef]
123. Sehested, K.; Corfitzen, H.; Fricke, H. The cobalt-60 γ-ray radiolysis of aqueous solutions of H_2 + O_2. Determination of $Ge^{-}{}_{aq}$ + G_H at pH 0.46–6.5. *J. Phys. Chem.* **1970**, *74*, 211–213. [CrossRef]
124. O'Donnell, J.H.; Sangster, D.F. *Principles of Radiation Chemistry*; American Elsevier Publishing Company: New York, NY, USA, 1970; pp. 80–98.
125. Bielski, B.H.J.; Cabelli, D.E.; Arudi, R.L.; Ross, A.B. Reactivity of HO_2/O_2^{-} radicals in aqueous solution. *J. Phys. Chem. Ref. Data* **1985**, *14*, 1041–1100. [CrossRef]
126. Pastina, B.; Isabey, J.; Hickel, B. The influence of water chemistry on the radiolysis of the primary coolant water in pressurized water reactors. *J. Nucl. Mater.* **1999**, *264*, 309–318. [CrossRef]
127. Marin, T.W.; Jonah, C.D.; Bartels, D.M. Reaction of $^{\bullet}OH$ radicals with H_2 in sub-critical water. *Chem. Phys. Lett.* **2003**, *371*, 144–149. [CrossRef]
128. Liu, G.; Du, T.; Toth, L.; Beninger, J.; Ghandi, K. Prediction of rate constants of important reactions in water radiation chemistry in sub- and supercritical water: Equilibrium reactions. *CNL Nucl. Rev.* **2016**, *5*, 345–361. [CrossRef]
129. Allen, A.O. *The Radiation Chemistry of Water and Aqueous Solutions*; D. Van Nostrand Co.: Princeton, NJ, USA, 1961.
130. Allen, A.O. The story of the radiation chemistry of water. In *Early Developments in Radiation Chemistry*; Kroh, J., Ed.; Royal Society of Chemistry, Thomas Graham House: Cambridge, UK, 1989; pp. 1–6.
131. Ingraham, L.L.; Meyer, D.L. *Biochemistry of Dioxygen*; Plenum Press: New York, NY, USA, 1985.
132. Halliwell, B.; Gutteridge, J.M.C. *Free Radicals in Biology and Medicine*; Oxford University Press: Oxford, UK, 2015.
133. Jay-Gerin, J.-P.; Ferradini, C. Are there protective enzymatic pathways to regulate high local nitric oxide ($^{\bullet}NO$) concentrations in cells under stress conditions? *Biochimie* **2000**, *82*, 161–166. [CrossRef]

134. Smith, D.R.; Stevens, W.H. Radiation-induced hydrolysis of acetal: Evidence for the reaction of H_3O^+ ions in spurs in the radiolysis of water. *Nature* **1963**, *200*, 66–67. [CrossRef]
135. Anbar, M.; Thomas, J.K. Pulse radiolysis studies of aqueous sodium chloride solutions. *J. Phys. Chem.* **1964**, *68*, 3829–3835. [CrossRef]
136. Schneider, N.M.; Norton, M.M.; Mendel, B.J.; Grogan, J.M.; Ross, F.M.; Bau, H.H. Electron-water interactions and implications for liquid cell electron microscopy. *J. Phys. Chem. C* **2014**, *118*, 22373–22382. [CrossRef]
137. Kanike, V.; Meesungnoen, J.; Jay-Gerin, J.-P. Acid spike effect in spurs/tracks of the low/high linear energy transfer radiolysis of water: Potential implications for radiobiology. *RSC Adv.* **2015**, *5*, 43361–43370. [CrossRef]
138. Islam, M.M.; Kanike, V.; Meesungnoen, J.; Lertnaisat, P.; Katsumura, Y.; Jay-Gerin, J.-P. *In situ* generation of ultrafast transient "acid spikes" in the $^{10}B(n,\alpha)^7Li$ radiolysis of water. *Chem. Phys. Lett.* **2018**, *693*, 210–215. [CrossRef]
139. Meesungnoen, J.; Jay-Gerin, J.-P.; Filali-Mouhim, A.; Mankhetkorn, S. Low-energy electron penetration range in liquid water. *Radiat. Res.* **2002**, *158*, 657–660. [CrossRef]
140. Lea, D.E. *Actions of Radiations on Living Cells*; Cambridge University Press: Cambridge, UK, 1946; Chapter 2.
141. Lea, D.E. The action of radiations on dilute aqueous solutions: The spatial distribution of H and OH. *Brit. J. Radiol.* **1947**, *1*, 59–64.
142. Morrison, P. Radiation in living matter: The physical processes. In *Symposium on Radiobiology. The Basic Aspects of Radiation Effects on Living Systems*; Nickson, J.J., Ed.; Wiley: New York, NY, USA, 1952; pp. 1–12.
143. Čerček, B.; Kongshaug, M. Hydrogen ion yields in the radiolysis of neutral aqueous solutions. *J. Phys. Chem.* **1969**, *73*, 2056–2058. [CrossRef] [PubMed]
144. Barker, G.C.; Fowles, P.; Sammon, D.C.; Stringer, B. Pulse radiolytic induced transient electrical conductance in liquid solutions. Part 1. Technique and the radiolysis of water. *Trans. Faraday Soc.* **1970**, *66*, 1498–1508. [CrossRef]
145. Pikaev, A.K.; Kabakchi, S.A.; Zansokhova, A.A. Yields and reactions of hydrogen ions on radiolysis of water and aqueous solutions. *Faraday Discuss. Chem. Soc.* **1977**, *63*, 112–123. [CrossRef]
146. Anderson, R.F.; Vojnovic, B.; Michael, B.D. The radiation-chemical yields of H_3O^+ and OH^- as determined by nanosecond conductimetric measurements. *Radiat. Phys. Chem.* **1985**, *26*, 301–303. [CrossRef]
147. Schmidt, K.H.; Ander, S.M. Formation and recombination of H_3O^+ and hydroxide in irradiated water. *J. Phys. Chem.* **1969**, *73*, 2846–2852. [CrossRef]
148. Byakov, V.M.; Stepanov, S.V. The mechanism for the primary biological effects of ionizing radiation. *Phys. Usp.* **2006**, *49*, 469–487. [CrossRef]
149. Kanike, V. "Acid-Spike" Effect in Spurs/Tracks of the Low/High Linear Energy Transfer Radiolysis of Water: Potential Implications for Radiobiology and Nuclear Industry. Master's Thesis, Université de Sherbrooke, Sherbrooke, QC, Canada, 2016. Available online: https://savoirs.usherbrooke.ca/handle/11143/9711 (accessed on 31 December 2024).
150. Meesat, R.; Belmouaddine, H.; Allard, J.-F.; Tanguay-Renaud, C.; Lemay, R.; Brastaviceanu, T.; Tremblay, L.; Paquette, B.; Wagner, J.R.; Jay-Gerin, J.-P.; et al. Cancer radiotherapy based on femtosecond IR laser-beam filamentation yielding ultra-high dose rates and zero entrance dose. *Proc. Natl. Acad. Sci. USA* **2012**, *109*, E2508–E2513. [CrossRef]
151. Kuppermann, A. Diffusion kinetics in radiation chemistry. In *Actions Chimiques et Biologiques des Radiations*; Haïssinsky, M., Ed.; Masson: Paris, France, 1961; Volume 5, pp. 85–166.
152. Burns, W.G.; Barker, R. Dose-rate and linear energy transfer effects in radiation chemistry. In *Progress in Reaction Kinetics*; Porter, G., Ed.; Pergamon: Oxford, UK, 1965; Volume 3, pp. 303–368.
153. Alanazi, A.; Meesungnoen, J.; Jay-Gerin, J.-P. A computer modeling study of water radiolysis at high dose rates. Relevance to FLASH radiotherapy. *Radiat. Res.* **2021**, *195*, 149–162. [CrossRef]
154. Fricke, H.; Morse, S. The chemical action of roentgen rays on dilute ferrosulphate solutions as a measure of dose. *Am. J. Roentgenol. Radium Ther.* **1927**, *18*, 430–432.
155. Fricke, H.; Morse, S. The action of X-rays on ferrous sulphate solutions. *Philos. Mag.* **1929**, *7th Ser. 7*, 129–141. [CrossRef]
156. Allen, A.O. Hugo Fricke and the development of radiation chemistry: A perspective view. *Radiat. Res.* **1962**, *17*, 255–261. [CrossRef]
157. Fricke, H.; Hart, E.J. Chemical dosimetry. In *Radiation Dosimetry*, 2nd ed.; Attix, F.H., Roesch, W.C., Eds.; Academic Press: New York, NY, USA, 1966; Volume II, pp. 167–239.
158. Allen, A.O. Radiation chemistry of aqueous solutions. *J. Phys. Colloid Chem.* **1948**, *52*, 479–490. [CrossRef] [PubMed]
159. Hochanadel, C.J.; Lind, S.C. Radiation chemistry. *Annu. Rev. Phys. Chem.* **1956**, *7*, 83–106. [CrossRef]
160. Klassen, N.V.; Shortt, K.R.; Seuntjens, J.; Ross, C.K. Fricke dosimetry: The difference between $G(Fe^{3+})$ for ^{60}Co γ-rays and high-energy X-rays. *Phys. Med. Biol.* **1999**, *44*, 1609–1624. [CrossRef]
161. McEwen, M.; El Gamal, I.; Mainegra-Hing, E.; Cojocaru, C. *Determination of the Radiation Chemical Yield (G) for the Fricke Chemical Dosimetry System in Photon and Electron Beams*; Report NRC-PIRS-1980; National Research Council Canada: Ottawa, ON, Canada, 2014.

162. International Commission on Radiation Units and Measurements. *The Dosimetry of Pulsed Radiation*; ICRU Report No. 34; International Commission on Radiation Units and Measurements: Bethesda, MD, USA, 1982.
163. Autsavapromporn, N.; Meesungnoen, J.; Plante, I.; Jay-Gerin, J.-P. Monte Carlo simulation study of the effects of acidity and LET on the primary free-radical and molecular yields of water radiolysis–Application to the Fricke dosimeter. *Can. J. Chem.* **2007**, *85*, 214–229. [CrossRef]
164. Tippayamontri, T.; Sanguanmith, S.; Meesungnoen, J.; Sunaryo, G.R.; Jay-Gerin, J.-P. Fast neutron radiolysis of the ferrous sulfate (Fricke) dosimeter: Monte Carlo simulations. *Recent Res. Dev. Phys. Chem.* **2009**, *10*, 143–211.
165. International Commission on Radiation Units and Measurements. *Radiation Dosimetry: X Rays and Gamma Rays with Maximum Photon Energies Between 0.6 and 50 MeV*; ICRU Report No. 14; International Commission on Radiation Units and Measurements: Washington, DC, USA, 1969.
166. Sehested, K.; Bjergbakke, E.; Holm, N.W.; Fricke, H. The reaction mechanism of the ferrous sulphate dosimeter at high dose rates. In *Dosimetry in Agriculture, Industry, Biology and Medicine, Proceedings of a Symposium on Dosimetry Techniques Applied to Agriculture, Industry, Biology and Medicine, Vienna, Austria, 16–20 April 1972*; International Atomic Energy Agency Publication STI/PUB/311; International Atomic Energy Agency: Vienna, Austria, 1973; pp. 397–404.
167. Běgusová, M.; Pimblott, S.M. Stochastic simulation of γ radiolysis of acidic ferrous sulfate solution at elevated temperatures. *Radiat. Prot. Dosim.* **2002**, *99*, 73–76. [CrossRef]
168. Sepulveda, E.; Sanguanmith, S.; Meesungnoen, J.; Jay-Gerin, J.-P. Evaluation of the radioprotective ability of cystamine for 150 keV–500 MeV proton irradiation: A Monte Carlo track chemistry simulation study. *Can. J. Chem.* **2019**, *97*, 100–111. [CrossRef]
169. Penabeï, S.; Meesungnoen, J.; Jay-Gerin, J.-P. Assessment of cystamine's radioprotective/antioxidant ability under high-dose-rate irradiation: A Monte Carlo multi-track chemistry simulation study. *Antioxidants* **2023**, *12*, 776. [CrossRef]
170. Ražem, D.; Miljanić, S.; Dvornik, I. Chemical dosimetry. In *Ionizing Radiation: Protection and Dosimetry*; Paić, G., Ed.; CRC Press: Boca Raton, FL, USA, 1988; pp. 157–186.
171. Trupin-Wasselin, V. Processus Primaires en Chimie Sous Rayonnement. Influence du Transfert d'Énergie Linéique sur la Radiolyse de l'Eau. Ph.D. Thesis, Université Paris XI, Orsay, France, 2000.